We are IntechOpen, the world's leading publisher of Open Access books Built by scientists, for scientists

6,900
Open access books available

186,000
International authors and editors

200M
Downloads

Our authors are among the

154
Countries delivered to

TOP 1%
most cited scientists

12.2%
Contributors from top 500 universities

WEB OF SCIENCE™

Selection of our books indexed in the Book Citation Index in Web of Science™ Core Collection (BKCI)

Interested in publishing with us?
Contact book.department@intechopen.com

Numbers displayed above are based on latest data collected.
For more information visit www.intechopen.com

6

Deconvolution Methods and Applications of Auditory Evoked Response Using High Rate Stimulation

Yuan-yuan Su, Zhen-ji Li and Tao Wang*
School of Biomedical Engineering, Southern Medical University
China

1. Introduction

An auditory-evoked potential (AEP) is electrophysiological activity within the auditory system that is stimulated by sounds. AEP components occurred at different latencies represent the regions giving rise to the responses in the auditory system. Accordingly, they are in general divided into three categories, i.e., early latency component, popularly known as auditory brainstem response (ABR), middle latency response (MLR) and later latency response (LLR). The AEP methodology has been widely used in assessing the functions of auditory system, and transmission of the electrical responses from the acoustic nerve via the brainstem to the cortex, which are associated with a series of timing different components lasting from about a few milliseconds up to several seconds. In clinic practice, AEPs, such as ABR in particular, are successfully applied to hearing screening for infants, identifying the organic or functional deafness; intraoperative monitoring for hearing preservation and restoration in acoustic surgery; intensive care unit monitoring of neurological status after severe brain injury, etc.

Due to the low-voltage nature of AEPs (microvolts level) recorded non-invasively at human scalp, distinct waveforms of AEPs have to be obtained by ensemble averaging technique, which requires hundreds or even thousands delivery of stimuli. The stimulus-intervals referred to as stimulus onset asynchrony (SOA) are inverse proportional to stimulus rates, which have to adapt to the response of interest in conjunction with the adjustment of band-pass filter settings to make sure that the duration of the transient waveform is shorter enough than that of SOA.

Many researches showed that high stimulus rates produce strong stresses on the auditory system which would benefit the diagnosis of the underlying disorders, and allow a more complete evaluation of auditory adaptation. It is reported that neuro-electrophysiological abnormalities in acoustic neuroma (Daly, 1977; Tanaka et al., 1996), multiple sclerosis (Robinson & Rudge, 1977), Bell's palsy (Uri et al., 1984) and mercury-exposed patients (Counter, 2003) are more evident and detectable under higher rate paradigms. It is also anticipated that higher rates might require less time to acquire observable responses (Bell et

* Corresponding author. Tel.: +86-20-61648276; E-mail: taowang@fimmu.com

al., 2001). However, the upper limit of the stimulus rate imposed by conventional ensemble averaging unfortunately restricts the application scopes that might be offered by the properties of rate effect. In general, one can study the responses under higher rate paradigms with uniform SOAs in terms of auditory steady state response (ASSR)—a periodic response, which can only be analyzed in frequency domain. For instance, the most investigated 40 Hz ASSRs first reported by Galambos et al. (1981), as the name indicated, are the responses to a stimulus rate at 40Hz.

One critical problem obstructs the application of high-rate stimulation is the overlapping of successive transient responses, which can be formulated mathematically as a convolution operation between the stimulus sequence and the response to individual stimulus (Jewett et al., 2004; Delgado & Ozdamar, 2004). The first technique attempted to unwrap the overlapped responses was proposed by Eyscholdt and Schreiner (1982), who employed a special family of binary impulse trains as stimuli. This method was soon widely used in the study of deriving ABRs in comparison with conventional paradigms in terms of morphology and recording efficiency (Burkard et al., 1990; Chan et al., 1992; Thornton & Slaven, 1993). In comparison with conventional ABR recording rate (maximum at 100 Hz), using MLS method, it is possible to obtain ABRs at stimulus rates up to 1000 Hz (Burkard et al., 1996a,b).

Stimulus trains of MLS must satisfy strict mathematic requirements. For example, the generation of MLS is implemented by using feedback shift registers, where the length of the binary train is solely determined by the memory number of register, moreover, the SOAs within a train must be multiples of a minimum pulse interval, which implies a wide range of jitters of SOA. Since neurosensory systems might exhibit different adaptation effects, the single derived AEP is in fact a kind of synthesis results of various responses to each stimulus. Recently, Ozdamar et al. (2004) and Jewett et al. (2004) developed similar techniques with a much lower SOA jittering to tackle this issue. These methods usually solve the convolution problem by an inverse filter in frequency domain, although it requires in practice that randomized SOAs in a stimulus sweep, the unwrapped responses, unlike in MLS paradigm, are sensitive to noise distribution along frequency bins within signal band. Wang et al. (2006) thus applied a Wiener filtering theory to attenuate amplified noise, if the power spectra of noise and signal can be estimated.

This chapter mainly focuses on introducing these techniques and applications using high stimulus rate paradigms. The rest of the chapter mainly consists of 5 Sections. Section 2 gives detailed descriptions to the theoretical framework of these techniques. Section 3 presents a simulated study on the comparison of recording efficiency using different paradigms. Section 4 proposes an iterative algorithm to the use of Wiener filter in the absence of spectral information of underlying response. Section 5 introduces applications of these techniques in clinics and practice. The conclusion with the future research directions are drawn in section 6.

2. Formulas of convolving responses and deconvolution techniques under high stimulus rates

Conventional averaging methods to obtain the transient responses assume that the response to a stimulus will be over or filtered out before next stimulus appears. Otherwise overlapped responses occur as illustrated in Fig. 1. This issue from the engineering point of

view, can be described as circular convolution of transient evoked response $x(t)$ and binary stimulus sequence $h(t)$. The convolution is defined as

$$y(t) = x(t) \otimes h(t) + n(t)\,, \tag{1}$$

where the symbol $\otimes$ denotes circular convolution operation. The noise $n(t)$ is assumed to be additive, which is independent with the transient evoked response $x(t)$. By the way, this model is also true for conventional case, where $x(t) \otimes h(t)$ is just a series of $x(t)$s time-locked to stimuli in $h(t)$, so that ensemble averaging is applicable as well.
The length of one period of $h(t)$ is called a sweep (see Fig.1(A)). There are usually more than eight stimuli with different SOAs in a sweep, which constitute a kind of complex stimulus presented repetitively so that conventional time-domain averaging can be carried out to obtain a noise-attenuated sweep-response as shown in Fig. 1(C). Unlike steady-state responses, the responses to all these individual stimuli appear different due to the degree of overlapping with varying SOAs. Deconvolution algorithms will thus make use of the information of such differences to estimate the underlying $x(t)$. Since additive noises may distort sweep-response, we thus conclude intuitively, that wide range SOA-jitters, such as MLS, will offer better anti-noise properties.

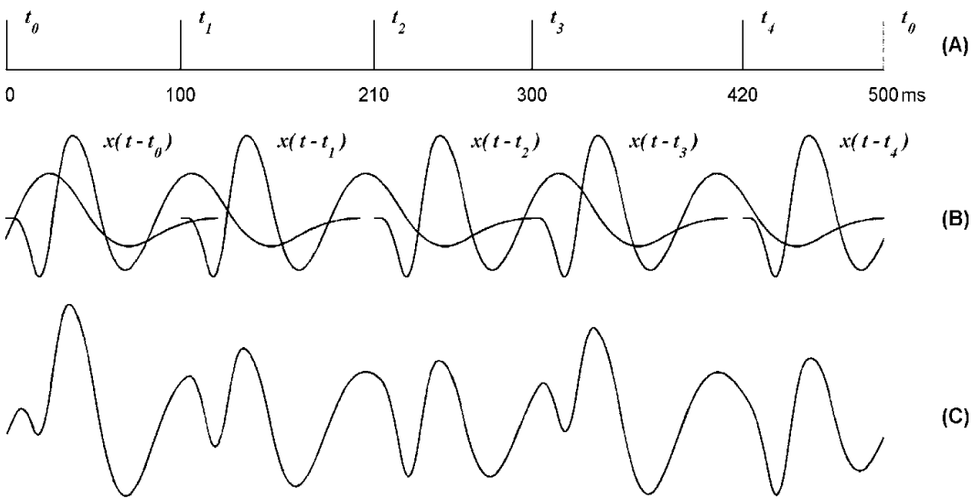

Fig. 1. Schematic illustration of deconvolution process. (A) Stimulus sequence with unequal SOAs. (B) Individual evoked response time-locked to stimuli onsets. (C) Overlapped response that is equivalent to convolution of stimulus sequence and individual evoked response.

2.1 Maximum length sequence (MLS) technique

An MLS train consists of an apparently random sequence of 0s and 1s that has a flat frequency spectrum for all frequencies. Unlike white noise, MLS trains are deterministic and therefore repeatable. It has been widely used in measuring the input impulse response of rooms for reverberation measurement.
MLS trains can be generated by a feedback shift register which is composed of binary memory elements that lined up and looped back through an operational element. The

number of memory elements is referred to as the order of MLS. An example in Fig.2 illustrates the generation of three order MLS trains. The binary state of a register is denoted by $s_i(j) \in \{0, 1\}$, where i = 1, 2, 3, in this case designating three memory elements, and j is equivalent to a timing index control, if in electronics, by a triggering clock. An important issue of MLS generation is the feedback state $b(j)$ to the very left element which is determined by a mathematic operation on the current states of elements. This operation is directly related to a primitive polynomial defined as $f(x) = x^3 + x + 1$ used in this case, where the term with the highest power (i.e., x^3) corresponds to the feedback state to $s_2(j)$, that is determined by two other elements, $s_1(j)$ indicated by term x, and $s_0(j)$ by term 1 (i.e., x^0) in $f(x)$, respectively. Specifically,

$$b(j) = [s_1(j) + s_0(j)] \bmod(2) . \tag{2}$$

A binary value in the MLS train is thus obtained from the output state of the right memory element $s_0(j)$. As long as one specifies the initial element states, $\{s_i(0)\}$, i = 1, 2, and 3, a periodic of MLS binary values, [a(0), a(1), …, a(6)] are thus produced one by one. For instance, if the initial state of the three memory elements is [1,1,1], the MLS train would be [1, 1, 1, 0, 0, 1, 0]. Varying the initial state is equivalent to circular shift of one period of MLS.

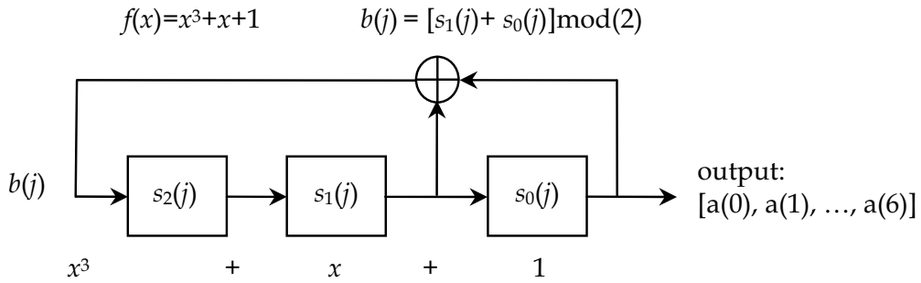

Fig. 2. Generation of three order MLS train by feedback shift register. $s_i(j)$ is the memory element of the feedback shift register, which is corresponding to the terms in primitive polynomial $f(x)$; symbol $\oplus$ stands for the calculation of feedback state $b(j)$; by specifying the initial element states, MLS binary values [a(0), a(1), …, a(6)] are produced one by one.

Conventionally, the 1 stands for a stimulus onset and 0 for the absence of a stimulus. Thus there are 2^{m-1} 1s indicating the total number of stimuli in a m-order MLS, and the total number of 0s and 1s in a period of MLS is referred to as the sequence length $L = 2^m - 1$. Therefore one can define minimum pulse interval (MPI) as a time interval between two adjacent values (1 or 0), for instance, '1-0' or '1-1' (see Fig. 3). Consequently, the SOAs must be multiples of the MPI. The SOA-jitter measured by the ratio between maximal SOA and minimal SOA for MLS is usually in the range of 4 ~ 6.

Replacing the term 0s with -1s, gives the recovery sequence $h_r(t)$. There is a specific relationship between the MLS stimulus and recovery sequences,

$$h_s(t) \otimes h_r(-t) = \frac{L+1}{2} \delta(t) . \tag{3}$$

Eq. (3) means that the circular convolution of the stimulus sequence $h_s(t)$ and the temporal reverse of recovery sequence $h_r(-t)$ is equal to the product of a delta function $\delta(t)$ and stimuli numbers in $h_s(t)$. As the overlap procedure explained in Eq.(1), the response evoked by $h_s(t)$ is modelled as

$$y(t) = x(t) \otimes h_s(t) , \tag{4}$$

of which convolving $h_r(-t)$ with both sides, it becomes

$$y(t) \otimes h_r(-t) = x(t) \otimes h_s(t) \otimes h_r(-t) . \tag{5}$$

Substituting with Eq. (3), and knowing that $x(t) \otimes \delta(t) = x(t)$, Eq.(5) becomes

$$y(t) \otimes h_r(-t) = \frac{L+1}{2} x(t) . \tag{6}$$

According to Eq.(6), overlapped signals can be unwrapped by convolving the observed response with the temporal reverse of MLS recovery sequence. The overall process of MLS paradigm is shown in Fig.3.

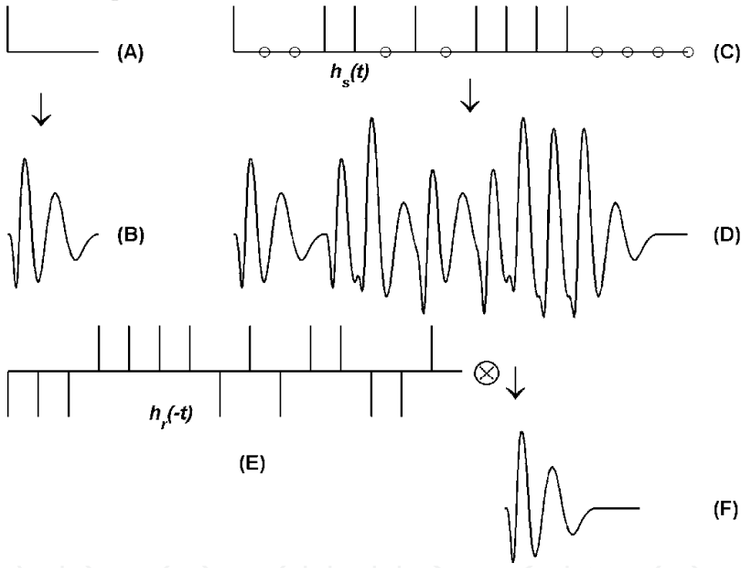

Fig. 3. Illustration of MLS paradigm. Single stimulus (A) evokes individual response (B). MLS with high stimulus rate (C) leads to overlapped sweep-response (D), which then convolves with the temporal reverse of recovery sequence (E) to retrieve the transient response (F).

2.2 Continuous loop averaging deconvolution (CLAD) technique

CLAD method was initially proposed to deconvolve the overlapped responses by matrix inverse in time domain (Delgado & Ozdamar, 2004). Similar to MLS, a sweep of stimulus $h(t)$ contains a sequence of stimuli with SOAs distributed in a random way. Mathematically, suppose $h(t)$ is binary column vector of length L, a square matrix can be constructed as

$$M = [h(t), h(t-1), h(t-2), ..., h(t-L)], \tag{7}$$

where $h(t - j)$, represent a time-lagged version of $h(t)$. Note that $h(t)$ is treated as a periodic sequence. The overlapped response $y(t)$ is thus formulated

$$y(t) = Mx(t). \tag{8}$$

The transient response $x(t)$ is obtained only if M is reversible.
An equivalent solution in frequency domain to this problem was also proposed later (Ozdamar et al., 2006). It is easy to derive that Eq.(8) is equivalent to a circular convolution model

$$y(t) = x(t) \otimes h(t), \tag{9}$$

which in frequency domain is $Y(f) = X(f)H(f)$, where the capital letters denote the Fourier transforms of the counterpart signals, and f denotes frequency in Hz. Therefore,

$$X(f) = \frac{Y(f)}{H(f)}. \tag{10}$$

It is obvious that calculation in frequency domain is faster than that in time domain. However, these mathematical models must be dealt with carefully in practice since the results might be highly distorted due to the presence of noise. Incorporating the additive background noise $n(t)$ into the Eq.(9), we get the same equation as Eq.(1). If we estimate $x(t)$ in frequency domain using Eq.(10), it can be further derived

$$\hat{X}(f) = \frac{Y(f)}{H(f)} = X(f) + \frac{N(f)}{H(f)} = X(f) + \frac{H^*(f)}{|H(f)|^2} N(f) \tag{11}$$

where the symbol * denotes the complex conjugate. It is easy to find out that the inverse filtering performs poorly in case that $H(f)$ has values smaller than unity, in which condition it will amplify the noise. Moreover, zeros (very small values due to digital quantification errors) in $H(f)$ at some frequencies will lead to overflow problem. This model suggests that the frequency properties of sweep stimulus $H(f)$ substantially affect the deconvolution performance. Usually sequences with lower jitters are especially susceptive to noise. Although, one can check a sequence's quality by its spectrum behaviour, it is unfortunately inconvenient for no theoretic solution to this optimal problem.
When the noise amplification problem exists for some stimulus sequences, an optimal algorithm in terms of mean square error (MSE) was proposed by Wang et al. (2006) using Wiener filtering theory. Base on Eq.(11), if the power spectra of noise and transient response can be estimated a priori, the optimal estimate becomes

$$\hat{X}(f) = W(f)Y(f) = \frac{H^*(f)}{|H(f)|^2 + P_n(f)/P_x(f)} Y(f) \tag{12}$$

where $W(f)$ is referred to as Wiener filter, $P_n(f)$ and $P_x(f)$ are power spectra of noise $n(t)$ and transient response $x(t)$, respectively. The ratio $P_n(f)/P_x(f)$, varies across frequency that tunes the Wiener filter to suppress those frequencies dominated by noise, and less affects the inverse filter, $1/H(f)$, in signal-dominated frequencies.

2.3 Q-sequence deconvolution

As mentioned above, if the jitter-ratio of SOAs is close to 1, i.e., the stimulus sequences are quasi-periodic, it is hard to find a "good" sequence which maintains noise attenuation property. Jewett et al. (2004) investigated this issue in very details and proposed a sophisticated criterion in the selection of a good sequence to accomplish the unwrapping task which was termed as quasi-periodic sequence deconvolution (QSD). Since the underlying responses are actually confined in a range of frequency band, it is workable to allocate the frequency band as passband f^P and stopband f^S. The sequences are selected so as to in the range of $f \in f^P$, that $H(f^P)$ satisfies the requirement of noise non-amplification. While in f^S, more attenuation measures apply. Retrieving transient response $x(t)$ under this framework is also carried out by combining two estimations from passband and stopband, respectively,

$$\{\hat{X}(f)\} = \{\hat{X}(f^p)\} \bigcup \{\hat{X}(f^s)\} . \tag{13}$$

By setting different filters—$H(f^P)$ and $S(f^S)$ for passband and stopband respectively, impact of stopband-noise can be reduced greatly. Substitute Eq. (11) to (13), respectively

$$\hat{X}(f^p) = \frac{X(f^p)H(f^p)}{H'(f^p)} + \frac{N(f^p)}{H'(f^p)} \tag{14}$$

$$\hat{X}(f^s) = \frac{X(f^s)H(f^s)}{S(f^s)} + \frac{N(f^s)}{S(f^s)} \tag{15}$$

where $H'(f^P)$ is usually identical with $H(f^P)$. The reason for distinguishing it is to provide an alternative if the users wish to adjust it under rare circumstances that fail to obtain the desired sequence. Adjustments may include changing values of $H(f)$ at specific frequencies so as to relief the corresponding noise amplification. The adjustment will of course affect the accuracy of waveform. Thus, careful assessment should be done beforehand.

2.4 Session-jittering deconvolution technique

There is one thing in common in the aforementioned deconvolution methods. The algorithm is associated with a sweep response $y(t)$ containing overlapped $x(t)$s. Jittered SOAs must be taken within a sweep of stimuli. However, many conventional AEP devices do not provide such flexible capability of user-defined stimuli. In the study for deconvolution of 40 Hz steady-state magnetic field responses, Gutschalk et al. (1999) adopted a jittering strategy using uniform SOAs in each recording session, while only gradually changed the SOAs in different recording sessions.

Suppose there are L sessions performed. Let $y_i(t)$, where sessional index i = 1, 2,…, L, be the response to equispaced stimuli $h_i(t)$, the corresponding SOA is denoted as T_i, and $x(t)$ be the transient response to an individual stimulus assumed identical for sessions, then $y_i(t) = h_i(t) \otimes x(t)$ as derived before. This model can also be expressed in matrix operation, i.e., $y_i = m_i x$, where binary matrix m_i is constructed by circular-shift versions of $h_i(t)$ in step-wise fashion. The row size of m_i is user defined which is at least larger than the length of $x(t)$. This process is the same as Eq. (7) except that $h_i(t)$ is equispaced.

Ideally, $y_i(t)$ is supposed to be a periodic steady-state response due to overlapping. By carrying out conventional ensemble averaging, gives one period of the overlapped response, $y_i(t)$, $t \in [0, T_i]$. This is equivalent to keep the column size of m_i to be T_i.

A sweep-like response $y(t)$ is formed by concatenating individual $y_i(t)$ one by one together,

$$y(t) = [y_1(t), y_2(t), ..., y_i(t)] = Mx(t) \ , \tag{16}$$

where $M = [m_1, m_2, \ldots, m_L]$. By applying the pseudo-inverse matrix M^{-1}, $x(t)$ can be retrieved. An illustration of this process is shown in Fig. 4. Note that the use of this method must be taken with care for the lack of discussions on noise effects. In fact, any matrix inverse calculation in practice might suffer the ill conditioning problem which is very sensitive to tiny disturbance.

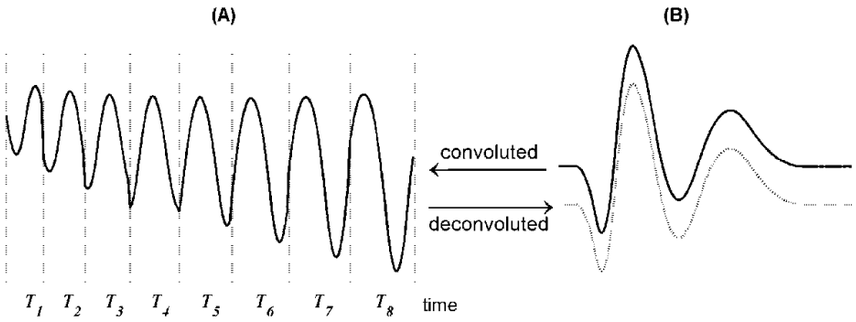

Fig. 4. The Simulation of session-jittering deconvolution. (A) Eight sessions of responses ($y_i(t)$) concatenate one by one according to a ascendant order of T_i. T_1~T_8 corresponding to SOAs increasing with a constant step-size represent length of individual $y_i(t)$. (B) Recovered response (dotted line) obtained by deconvolution is identical with original response (solid line).

3. Recoding efficiency with high rate stimulation

Given the same number of stimulus, people expect that high rate stimulation would reduce the recording time, and the signal to noise ratio (SNR) for high rate paradigm would remain comparable with conventional counterpart. However, since the number of sweep for high rate approach is reduced by a factor of L (where L is the number of stimuli in a sweep), sweep averaged responses do not necessarily offer better SNR than conventional ones. In the processing stage of deconvolution, there are however, still chances to either improve or deteriorate SNR depending on the characteristics of sequences. Consequently, it is essential to evaluate the efficiency of these high rate paradigms in deconvolving evoked responses.

A simulated comparison among three paradigms— conventional ensemble averaging, MLS and CLAD is performed. The comparison processes are illustrated in Fig.5. First, an ideal response which convolves with a preset sequence is generated, and then both ideal and overlapped responses are added with the same level noises. The transient responses are obtained by conventional, MLS and CLAD paradigms respectively, and recording efficiencies are evaluated by measuring the correlation coefficients (CCs) and mean square errors (MSEs) of ideal and transient responses.

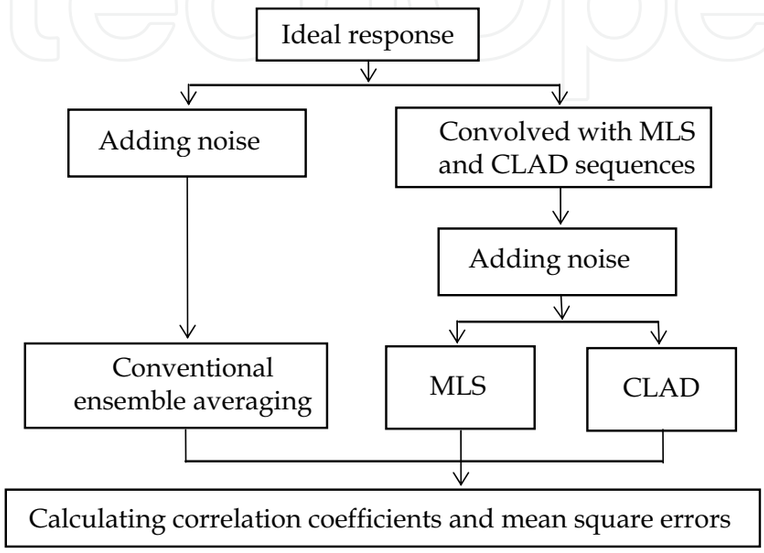

Fig. 5. The flowchart of comparison procedure of recording efficiency

For the convenience of following elaborations, we set up an artificial sampling rate of 1000 Hz. The parameters settings are as followings. The effective length of ideal response lasts 200 ms, which is composed of 5 components with different latencies, amplitudes and polarities (see Fig. 6). Background noises like EEG are modelled by pink noise—a kind of noise generally found in complex system with $1/f$ power spectra. A five order MLS sequence {1 0 0 1 0 1 1 0 0 1 1 1 1 1 0 0 0 1 1 0 1 1 1 0 1 0 1 0 0 0 0} and a lower-jittering Q-sequence (from Jewett et al., 2006) {1 5595 12228 18525 24220 29435 35394 41904 47133 53749 59088 64479 71112} are defined as fundamental sequences. These sequences are in essential dimensionless. These fundamental sequences are stretched or compressed proportionally to form 11 sequences with stimulus rates from 8 S/s (stimulus per second) to 48 S/s (i.e., step-size 4S/s), respectively. Corresponding SOAs in this range are shorter than ideal response, so that overlapping in observed signals occurs. The reason of using different rates is that the performance of deconvolution might be relevant to overlapping degrees.
The performance is evaluated by averaged CCs and MSEs over 20 runs (defined as each simulation with one mixture of noise). For different stimulus rates, the sweep numbers are adjusted to make approximately the same recording time.
As illustrated in Fig.6, the MLS response is quite similar to ideal response not only in latencies and amplitudes of their waves but in their morphology. However, there is more morphological distortion in CLAD response. Both MLS and conventional responses are

more approximate to the ideal one. The MLS method seems more efficient in higher stimulus rates, under the condition of the same recording time.

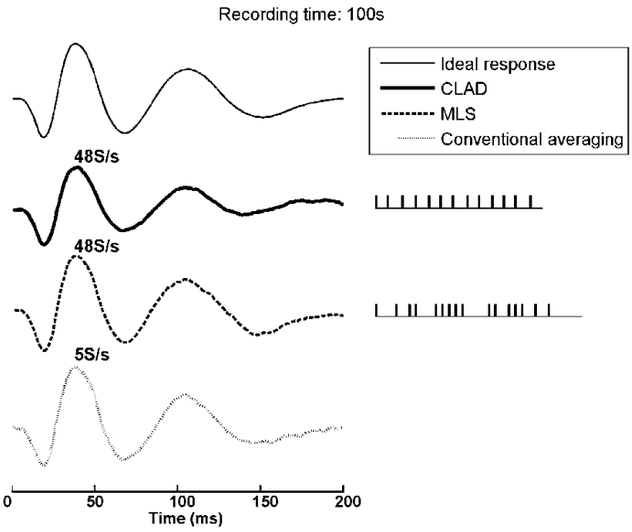

Fig. 6. Retrieved AEPs by CLAD, MLS and conventional methods indicated by legend. Stimulus sequences of CLAD and MLS are placed on the right, respectively.

Fig.7 shows the performance measured with CCs and MSEs. There is a sudden decline in correlation coefficient curve of CLAD indicating the inefficiency at some rates. The cause of this decline is not yet known. We speculated that it may be related to the different superposition enhancements at certain rates, since we observed that the amplitudes of overlapped responses were decreased at these rates.

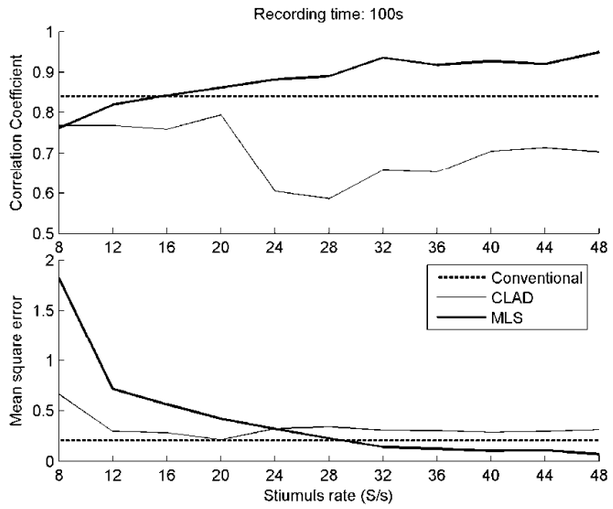

Fig. 7. CCs and MSEs at different stimulus rates, under 100 s recording time.

It is expected that MLS is better than CLAD with lower jitters under the same noise environment. The characteristic of CLAD's sweep-response is more like steady-state

response than that of MLS (Fig.8), implying less recovery information available. It implies that the key in high rate paradigms lies in deconvolving the overlapped responses; merely increasing stimulus rates for lower jittered sequences may not be used as a means to improve the recording efficiency.

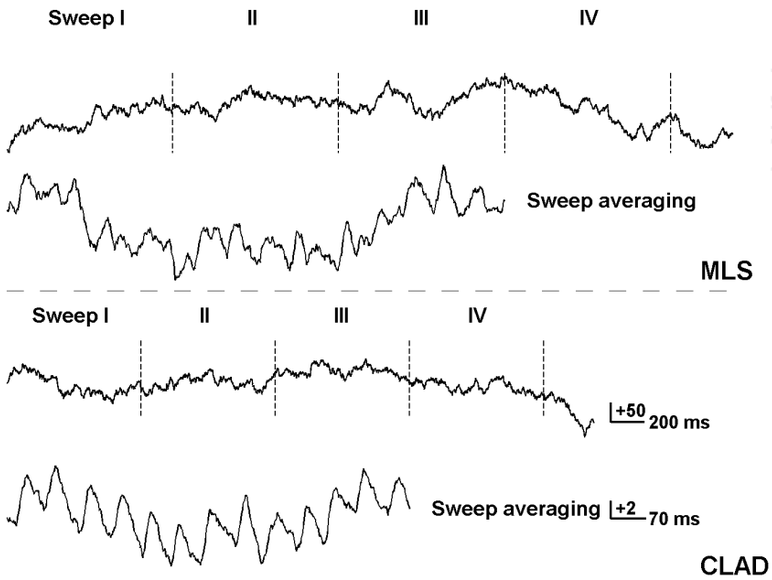

Fig. 8. Averaged sweep-responses for MLS and CLAD in the simulation. Row one and three are raw EEGs, row two and four are sweep-responses

4. Iterative Wiener filtering method

Wiener filtering has been successfully used to tackle the noise amplification problem taking place at a few frequencies bins for some lower jittered sequences (Wang et al., 2006). If the power spectra of both noise and signal are estimated correctly, the inverse filter will be able to adapt to the ratio of noise and signal in frequency domain. In general applications, estimation of signal power spectrum is not readily available in comparison with that of noise. Therefore, a method for evaluating power spectra of transient response by long term memory iterative algorithm is proposed. Fig. 9 depicts the iterative process.

First, initial value $K(f)$, say a constant unity, and adjusted factor c are preset, so the initial transient response $X_0(f)$ is recovered by Eq.(12). Assuming the power spectrum of background noise is constant, and all the estimated responses are kept and averaged to estimate power spectra of response used for next iterative calculation. If the difference of two successive estimates of $x(t)$ measured by the relative Euclidean norm is smaller than a given arbitrary minimum positive, iteration stops, otherwise repeat the iteration.

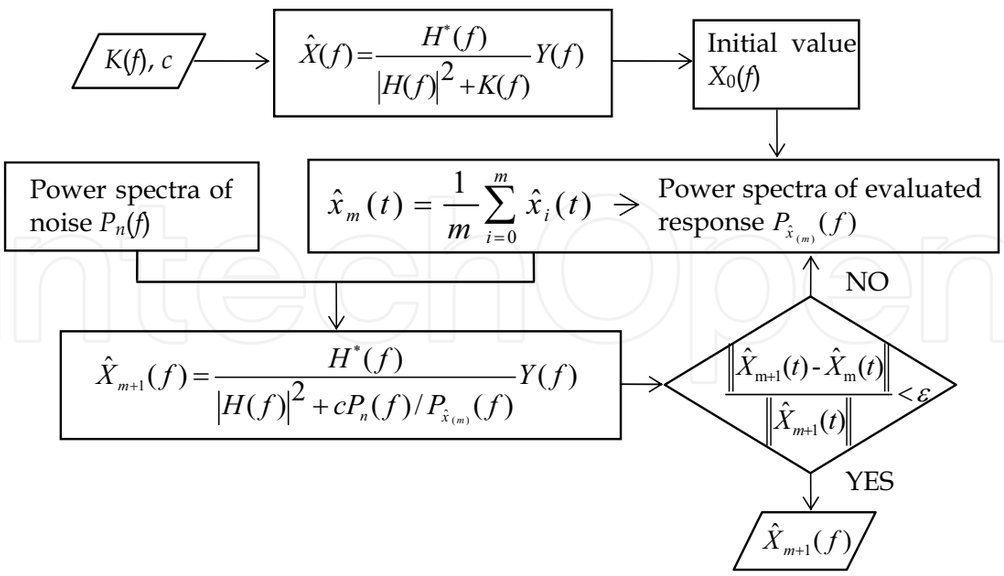

Fig. 9. Flowchart of iterative process.

In simulation data, the ideal response and additive noise are identical with that used in Section 3, and the stimulus sequence which rate is 24 S/s lasts 535 ms. The real data come from Wang's experiment (Wang et al., 2006), the rate of stimulus sequence is also 24 S/s. This sequence lasts 205ms. Both sequences have similar parameters. In order to determine the convergence of this iterative algorithm, the correlation coefficients (CCs) of present and the ideal responses are calculated. The theoretical CC in the simulation study is calculated by using the known signal power spectrum rather than the estimated ones. The parameter *c* (range 0~1) is introduced to weight the proportion of *K*(*f*), when in the presence of strong artefacts, larger *c* could alleviate their effects.

The simulation results are shown in Fig. 10. The waveform obtained from the proposed algorithm (solid trace in panel D) is close to the theoretical one (doted trace). It is obvious that *K*(*f*) will affect both noise and signal, the estimated responses are bias and the magnitudes tend to be suppressed.

The correlation coefficient curve also shows that the estimations (indicated by symbol *) are gradually approaching to the theoretical estimation (dash line).

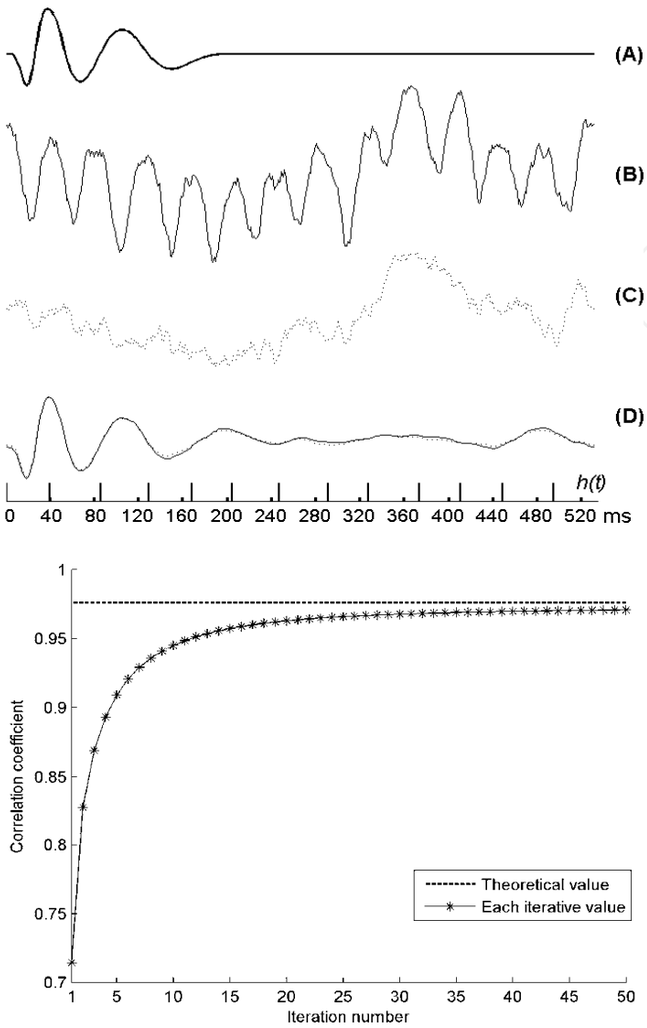

Fig. 10. Top panel shows the ideal AEP (A), sweep response (B) with the corresponding noise (C). A comparison of retrieved AEPs (D) using iterative algorithm (solid) and theoretic one (dotted). Bottom panel shows the CCs for iterative algorithm and the theoretical one.

The performance of the proposed algorithm using human recorded data as in (Wang et al., 2006) is shown in Fig.11. The very weak AEPs are buried in raw EEG and large noises, and it is hard to identify them even in the averaged sweep. However, after estimating residual noise as the background noise by ± reference method (Schimmel, 1967), the power spectra of noise are calculated and the iterative estimation can proceed. This iterative method attenuates noise greatly and highlights the feature waves V~P_1 out of raw EEG.

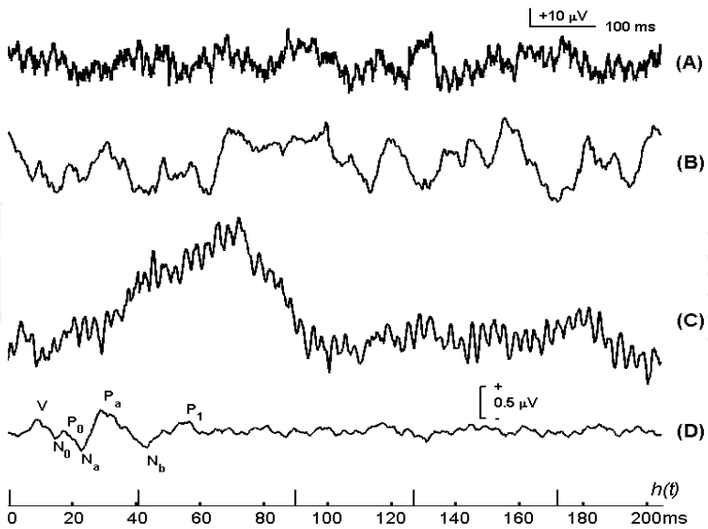

Fig. 11. Real data-processing results. (A) Raw EEG; (B) EEG processed by ± reference method; (C) Estimated residual noise; (D) Iterative recovered waveform.

The drawback of the algorithm is that there is no theoretic analysis of the convergent property. To ensure the iterative algorithm convergent in line with the correct direction, attention has to be paid to the initial states of the algorithm. If $K(f)$ is constant, signal and noise are suppressed the same over all the frequency band. The purpose of iteration is to adjust the suppression factor $K(f)$ based on the spectrum of the estimated signal. Usually at the initial stage, using a relative larger $K(f)$ will guarantee sufficient noise attenuation, although the estimated signal is also attenuated. Since the noise is more wide-band, a larger attenuation of both signal and noise is more likely to produce a better SNR signal estimation, which is able to yield a correct step-forward adjustment of $K(f)$ for next iteration.

5. Applications of high rate techniques in clinical and basic researches

Since the proposal of deconvolution techniques for high-rate stimulation, especially the early developed MLS method, researchers have been exploring the possible applications in various areas. In the study of ABR, it has been noticed that reliable ABRs were produced remarkably comparable to conventional ones in morphology (Burkard et al., 1990).

During recording ABR of premature infants by MLS, Weber and Roush (1993) found that the clarity of ABR could be well-defined under a rate as high as of about 900 S/s and the quality of MLS-ABR was even better than conventional ABR especially in large noise environment. It suggested that MLS could be applied in newborn hearing screening. This suggestion was also verified by Jiang et al. (Jiang et al., 1999). Besides, they also employed MLS in asphyxiated neonates and found that the central auditory impairment of these neonates was more detectable with this paradigm (Jiang et al, 2001).

Although MLS can raise the stimulus rate up to 1000 S/s, the rate is not the higher the better, due to adaptation effects. Thornton and Slaven (1993) found that SNR of ABR recording improved with increasing rate and came to a stop at 200 S/s, and then further increasing the

rate would lead to worsening performance. Leung et al. (1998) also verified that the optimal MLS rate was in the range of 200~300 S/s during estimation of hearing threshold.

In the study of MLRs, Musiek and Lee (1997) concluded that no clear diagnostic advantage was shown for using MLS technique in patients with central nervous system lesions. While Bell et al. (2001) found that MLS could produce better wave identification and recording efficiency. Their study showed that MLS appears to produce greater improvement in recording speed for the P_a-N_b segment of the MLR than for the N_a-P_a segment, which might imply that different regions of the auditory pathway are responsible for producing the two segments of MLR. In their recently pilot study (Bell et al., 2006), MLS stimulation in conjunction with chirp stimulus sound were investigated in studying MLR variance as a potential indicator for anesthesia adequacy.

With the recently developed methods with lower-jittered sequences, CLAD or QSD paradigms are gradually applied in many studies. For instance, CLAD was implemented with other denoising techniques to assess MLRs recorded during sleep and the relation of MLRs and sleep stages was reported (Millan et al., 2006). Since the auditory MLR as well as the 40-Hz ASSR are both applicable to indicate anesthesia, the deconvolution techniques offer a way to study the relationship between the MLRs and transient ASSR during general anethesia (McNeer et al., 2009). It is found that the morphology of the transient ASSR is dependent on the stimulus rates during anesthesia. By employing CLAD to unwrap the ASSR, it was found that there was dramatic increase in amplitude of P_b component at 40 Hz and suggested that may account for the high amplitude of 40Hz-ASSR (Ozdamar et al., 2007). A further research on 40 Hz ASSR (Bohorquez & Ozdamar, 2008) also showed that the 40 Hz ASSR is a composite response mainly overlapped by ABR and MLR, and the high amplitude of ASSR at 40 Hz results from the superposition of P_b component to P_a wave.

The QSD method was also applied for investigating auditory transient ASSR which was called “G-wave” by quasi-periodic tone-pip stimulus sequences presented at 40 Hz (Larson-Priora et al., 2004). The recent finding has extended high rate techniques to other modalities, such as visual and somatosensory stimulation (Jewett et al, 2006). In this finding, they recorded a type of oscillatory waves named A-waves in the alpha rhythmic range, and found that there was a sensation-transition zone implying a range of certain stimulus rates in which the sensation of individual stimuli fuse into a continuity. Stimulus rates above and below this zone could lead to systematic differences in shape of A-wave, and the waveforms evoked above and below this zone may relate to two neuronal processing modes called “flash-memory” and “fusion-memory” respectively. They speculated that A-wave was a new evoked response phenomenon which may provide a way to reveal the mechanism of neural processing.

6. Conclusion

Despite the strong evidence of the benefits of using high-rate stimulation, technical difficulties prevent it from widespread applications in clinics. In this chapter we did an extensive literature survey on the subject of deconvolution of high rate AEPs. These techniques allow the study of more rang of rate-effects, such as ABRs up to 1000 Hz (S/s), and also allow exploring transient properties of steady-sate responses in time domain. Clinical applications are also showing a great promising in recent anesthesia investigation.

The fundamental idea behind all the techniques lies in the jittering strategy of the stimulus sequences. Unfortunately there is still no theoretical solution to the problem of finding an optimal sequence under lower jitter condition. Moreover, current methods are sill unable to deal with multivariate cases in other popular paradigms, such as oddball, where there are more than one transient response exist.

7. Acknowledgements

We would like to thank Drs. Ozdamar and Bohorque for offering valuable materials and comments. This work was supported by National Science Foundation of China (No. 60771035).

8. References

Bell, S.L.; Allen, R. & Lutman, M.E. (2001). The feasibility of maximum length sequences to reduce acquisition time of the middle latency response. *The Journal of Acoustical Society of America*, Vol. 109, No. 3, 1073-1081

Bell, S.L.; Smith, D.C.; Allen, R. & Lutman, M.E. (2006). The auditory middle latency response, evoked using maximum length sequences and chirps, as an indicator of adequacy of anesthesia. *Anesthesia and Analgesia*, Vol. 102, No. 2, 495-498

Bohorquez, J. & Ozdamar, O. (2008). Generation of the 40-Hz auditory steady-state response (ASSR) explained using convolution. *Clinical Neurophysiology*, Vol. 119, No. 11, 2598-2607

Burkard, R.; Shi, Y. & Hecox, K.E. (1990). A comparison of maximum length and Legendre sequences for the derivation of brain-stem auditory-evoked responses at rapid rates of stimulation. *The Journal of Acoustical Society of America*, Vol. 87, No. 4, 1656-1664

Burkard, R.; McGee, J. & Walsh, E. (1996a). The effects of stimulus rate on the feline BAER during development, I. Peak latencies. *The Journal of Acoustical Society of America*, Vol. 100, No. 2, 978-990

Burkard, R.; McGee, J & Walsh, E. (1996b). The effects of stimulus rate on the feline BAER during development, II. Peak amplitudes. *The Journal of Acoustical Society of America*, Vol. 100, No. 2, 991-1002

Chan, F.H.; Lam, F.K.; Poon, P.W. & Du, M.H. (1992). Measurement of human BAERs by the maximum length sequence technique. *Medical and Biological Engineering and Computing*, Vol. 30, No. 1, 32-40

Counter, S.A. (2003). Neurophysiological anomalies in brainstem responses of mercury-exposed children of Andean gold miners. *Journal of Occupational and Environmental Medicine*, Vol. 45, No. 1, 87-95

Daly, D.; Roeser, R.; Aung, M. & Daly, D.D. (1977). Early evoked potentials in patients with acoustic neuroma. *Electroencephalograph and Clinical Neurophysiology*, Vol. 43, No. 2, 151-159

Delgado, R.E. & Ozdamar, O. (2004). Deconvolution of evoked responses obtained at high stimulus rates. *The Journal of Acoustical Society of America*, Vol. 115, No. 3, 1242-1251

Eysholdt, U. & Schreiner, C. (1982). Maximum length sequences--A fast method for measuring brainstem-evoked responses. *Audiology*, Vol. 21, No. 3, 242-250

Galambos, R.; Makeig, S. & Talmachoff, P.J. (1981). A 40-Hz auditory potential recorded from the human scalp. *Proceedings of the National Academy of Sciences*, Vol. 78, No. 4, 2643-2647

Gutschalk, A.; Mase, R.; Roth, R.; Ille, N.; Rupp, A.; Hahnel, S.; Picton, T.W. & Scherg, M. (1999). Deconvolution of 40 Hz steady-state fields reveals two overlapping source activities of the human auditory cortex. *Clinical Neurophysiology*, Vol. 110, No. 5, 856-868

Jewett, D.L.; Caplovitz, G.; Baird, B.; Trumpis, M.; Olson, M.P. & Larson-Prior, L.J. (2004). The use of QSD (q-sequence deconvolution) to recover superposed, transient evoked-responses. *Clinical Neurophysiology*, Vol. 115, No. 12, 2754-2775.

Jewett, D.L.; Hart, T.; Baird, B.; Larson-Prior, L.J.; Baird, B.; Olson, M.; Trumpis, M.; Makayed, K. & Bavafa, P. (2006). Human sensory-evoked responses differ coincident with either "fusion-memory" or "flash-memory", as shown by stimulus repetition-rate effects. *BMC Neuroscience*, Vol. 7, available at http://www.biomedcentral.com /1471-2202/7/18

Jiang, Z.D.; Brosi, D.M. & Wilkinson, A.R. (1999). Brainstem auditory evoked response recorded using maximum length sequences in term neonate. *Biology of the Neonate*, Vol. 76, No. 4, 193-199

Jiang, Z.D.; Brosi, D.M. & Wilkinson, A.R. (2001). Comparison of brainstem auditory evoked responses recorded at different presentation rates of clicks in term neonates after asphyxia. *Acta Paediatrica*, Vol. 90, No. 12, 1416-1420

Larson-Prior, L.J.; Hart, M.T. & Jewett, D.L. (2004). Neural processing of high-rate auditory stimulation under conditions of various maskers. *Neurocomputing*, Vol. 58-60, 993-998

Leung, S.M.; Slaven, A.; Thornton, A.R. & Brickley, G.J. (1998). The use of high stimulus rate auditory brainstem responses in the estimation of hearing threshold. *Hearing research*, Vol. 123, No. 1-2, 201-205

McNeer, R.R.; Bohorquez, J. & Ozdamar, O. (2009). Influence of auditory stimulation rates on evoked potentials during general anesthesia: relation between the transient auditory middle-latency response and the 40-Hz auditory steady state response. Anesthesiology, Vol. 110, No. 5, 1026-1035

Millan, J.; Ozdamar O. & Bohorquez J. (2006). Acquisition and analysis of high rate deconvolved auditory evoked potentials during sleep. *Proceedings of Engineering in Medicine and Biology Society*, Vol. 1, 4987-4990

Musiek, F.E. & Lee, W.W. (1997). Conventional and maximum length sequences middle latency response in patients with central nervous system lesions. *Journal of the American Academy of Audiology*, Vol. 8, No. 3, 173-180

Ozdamar, O. & Bohorquez, J. (2006). Signal-to-noise ratio and frequency analysis of continuous loop averaging deconvolution (CLAD) of overlapping evoked potentials. *Journal of Neuroscience Methods*, Vol. 119, No. 1, 429-438

Ozdamar, O.; Bohorquez, J. & Ray, S.S. (2007). P(b)(P(1)) resonance at 40 Hz: effects of high stimulus rate on auditory middle latency responses (MLRs) explored using deconvolution. *Clinical Neurophysiology*, Vol. 118, No. 6, 1261-1273

Robinson, K. & Rudge, P. (1977). Abnormalities of the auditory evoked potentials in patients with multiple sclerosis. *Brain*, Vol. 100, 19-40

Schimmel, H. (1967). The ± reference: accuracy of estimated mean components in average response studies. *Science*, Vol. 157, No. 784, 92-94

Tanaka, H.; Komatsuzaki, A. & Hentona, H. (1996). Usefulness of auditory brainstem responses at high stimulus rates in the diagnosis of acoustic neuroma. *Journal of Oto-Rhino- Laryngology and its Related Specialties*, Vol. 58, No. 4, 224-228

Thornton, A.R. & Slaven, A. (1993). Auditory brainstem responses recorded at fast stimulation rates using maximum length sequences. *British journal of audiology*, Vol. 27, No. 3, 205-210

Wang, T.; Ozdamar, O.; Bohorquez, J.; Shen, Q. & Cheour, M. (2006). Wiener filter deconvolution of overlapping evoked potentials. *Journal of Neuroscience Methods*, Vol. 158, No. 2, 260-270

Weber, B.A. & Roush, P.A. (1993). Application of maximum length sequence analysis to auditory brainstem response testing of premature newborns. *Journal of the American Academy of Audiology*, Vol. 4, No. 3, 157-162

Uri, N.; Schuchman, G. & Pratt, H. (1984). Auditory brain-stem evoked potentials in Bell's palsy. *Archives of otolaryngology*, Vol. 100, No. 5, 301-304

IntechOpen

New Developments in Biomedical Engineering
Edited by Domenico Campolo

ISBN 978-953-7619-57-2
Hard cover, 714 pages
Publisher InTech
Published online 01, January, 2010
Published in print edition January, 2010

Biomedical Engineering is a highly interdisciplinary and well established discipline spanning across engineering, medicine and biology. A single definition of Biomedical Engineering is hardly unanimously accepted but it is often easier to identify what activities are included in it. This volume collects works on recent advances in Biomedical Engineering and provides a bird-view on a very broad field, ranging from purely theoretical frameworks to clinical applications and from diagnosis to treatment.

How to reference
In order to correctly reference this scholarly work, feel free to copy and paste the following:

Yuan-yuan Su, Zhen-ji Li and Tao Wang (2010). Deconvolution Methods and Applications of Auditory Evoked Response Using High Rate Stimulation, New Developments in Biomedical Engineering, Domenico Campolo (Ed.), ISBN: 978-953-7619-57-2, InTech, Available from: http://www.intechopen.com/books/new-developments-in-biomedical-engineering/deconvolution-methods-and-applications-of-auditory-evoked-response-using-high-rate-stimulation

INTECH
open science | open minds

InTech Europe
University Campus STeP Ri
Slavka Krautzeka 83/A
51000 Rijeka, Croatia
Phone: +385 (51) 770 447
Fax: +385 (51) 686 166
www.intechopen.com

InTech China
Unit 405, Office Block, Hotel Equatorial Shanghai
No.65, Yan An Road (West), Shanghai, 200040, China
中国上海市延安西路65号上海国际贵都大饭店办公楼405单元
Phone: +86-21-62489820
Fax: +86-21-62489821

© 2010 The Author(s). Licensee IntechOpen. This chapter is distributed under the terms of the Creative Commons Attribution-NonCommercial-ShareAlike-3.0 License, which permits use, distribution and reproduction for non-commercial purposes, provided the original is properly cited and derivative works building on this content are distributed under the same license.

IntechOpen

IntechOpen